INTERNATIONAL JOURNAL OF CLIMATOLOGY
Int. J. Climatol. **33**: 2836–2845 (2013)
Published online 5 December 2012 in Wiley Online Library
(wileyonlinelibrary.com) DOI: 10.1002/joc.3630

RMetS
Royal Meteorological Society

Connections of ENSO/IOD and aerosols with Thai rainfall anomalies and associated implications for local rainfall forecasts

Arika Bridhikitti*

Faculty of Environment and Resource Studies, Mahasarakham University, Maha Sarakham, Thailand

ABSTRACT: El Niño/La Niña Southern Oscillation (ENSO), Indian Ocean Dipole (IOD) and aerosols have important roles to play in relation to Southeast Asian rainfall anomalies. This study investigates connections between these factors and local seasonal rainfall anomalies at 17 locations throughout Thailand using ground measurements and satellite observations available from 1980 to October 2011. This research investigates further the usefulness of incorporating these factors into rainfall forecasts. Results from canonical correlation analysis indicate that strong ENSO signals from October to March may affect rainfall anomalies in the nonsummer monsoon months, whereas IOD signals in the previous summer monsoon months were deemed to be of greater responsibility for current summer monsoon rainfall. Comparison of rainfall levels with different aerosol loadings suggests rainfall-decreasing aerosol from December to February for the South East Coast and in pre-summer monsoon months for deeper inland areas having less coastal influences. Rainfall-increasing aerosol was observed in post-summer monsoon months at the inland stations. The use of ENSO/IOD signals as predictors yielded better rainfall forecast model performance than that of the aerosol loading. However, model performance significantly improved when both ENSO/IOD signals and seasonal aerosol loadings were introduced.

KEY WORDS biomass burning aerosol; climate of Thailand; dipole mode index; ENSO; Indian Ocean Dipole; rainfall anomalies; sulphate aerosol

Received 17 April 2012; Revised 1 September 2012; Accepted 31 October 2012

1. Introduction

In Thailand, rainfall is a major source of water which is primarily used for agricultural production. Reliable rainfall forecasts, therefore, are beneficial for agricultural water management. The capability of the forecast model is, however, limited by current understanding of long- and short-term rainfall variation trends and latent factors forcing local rainfall changes. These factors include El Niño/La Niña Southern Oscillation (ENSO), Indian Ocean Dipole (IOD) and aerosols.

Without ENSO/IOD effects, periods of the above and below normal rainfall in Thailand last about one to three decades (Kripalani and Kulkarni, 1997). ENSO amplifies the above and below normal rainfall causing inundation and extreme drought (Kripalani and Kulkarni, 1997). Singhrattna *et al.* (2005a) found that the Southern Oscillation Index (SOI) has a stronger positive relationship with Thai rainfall statistics from August to October after 1980, when El Niño tends to decrease the rainfall through weakening Walker circulation over the Thailand–Indonesian region. Their research further suggests using SOI-based predictors for Thai monsoon rainfall forecasts (Singhrattna *et al.*, 2005b). Chansaengkrachang *et al.* (2011) shows evidence of IOD affecting the variability of corresponding Thai rainfall. ENSO/IOD feedback to local seasonal rainfall, ENSO/IOD co-effects and time lag between IOD signals to rainfall response are, however, not well discussed in these works.

The absorption and/or scattering of sunlight by atmospheric aerosols tend to modify the climate. Some aerosols also act as cloud condensation nuclei. Both aerosol effects are dependent on the physiochemical characteristics of aerosols and are proven to induce changes in rainfall patterns (Mitchell and Johns, 1997; Ramanathan *et al.*, 2001; Ramanathan *et al.*, 2005; Meehl *et al.*, 2008). The results from the global climate model simulation shows that sulphate aerosol may reverse increasing Southeast Asian rainfall trends induced by greenhouse gases (Mitchell and Johns, 1997). This sulphate aerosol is attributed to burning fossil fuels, largely in the Southeastern China (Bridhikitti and Overcamp, 2011). This sulphate aerosol scatters sunlight and cools the Earth's surface and atmosphere. Black carbon aerosol may oppose the cooling effect of the sulphate aerosol at the top of atmosphere, whereas at the surface all aerosols play a

* Correspondence to: A. Bridhikitti, Faculty of Environment and Resource Studies, Mahasarakham University, Muang, Maha Sarakham 44000, Thailand. E–mail: arika.b@msu.ac.th

cooling role. Climate effects in response to black carbon aerosol are dependent on local ground–atmosphere interaction processes (Ramanathan *et al.*, 2001). The model simulation also shows that black carbon aerosol, largely from agricultural open burning emissions (Bridhikitti and Overcamp, 2011), is cooling the Earth's surface and subsequently decreasing presummer monsoon rainfall over Thailand (Meehl *et al.*, 2008). There are very few observation-based studies confirming these aerosols' effects on the rainfall levels. Lau and Kim (2006) have found increasing rainfall anomaly trends over most Thai territory, but the connection between these trends and local aerosols is not discussed in their work. This study provides evidence from ground measurements and satellite observations showing Thai rainfall–aerosol connections.

The objectives of this study are (1) to understand the common climate structure of Thailand from 1980 to 2011, (2) to show the connections of ENSO/IOD and aerosols with local seasonal rainfall anomalies in Thailand and (3) to investigate the usefulness of incorporating these rainfall-inducing factors as predictors for rainfall forecasts.

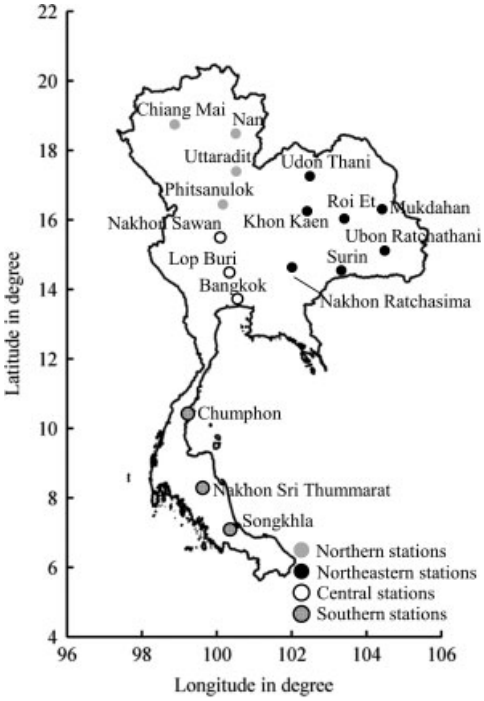

Figure 1. Thailand meteorological stations considered in this study.

2. Methodology

2.1. Description of studied locations

Thailand, located in Southeast Asia, is potentially affected by both ENSO from the tropical Pacific Ocean and IOD. The Northern and Northeastern parts of the country, being deeper inland, are less affected by coastal influences. Forests are abundant in the North and deforestation here is also significant (Walker, 2002). Flat highlands in the NE stations are primarily covered with rice paddies. This land contributes high aerosol loading to the atmosphere during the agricultural burning season from February to May. The Central region includes the capital, Bangkok. The climate here may be influenced by land–sea circulation, urban heat island and contributions from urban and agricultural activities. The Southern region consists of Peninsular and Archipelago geographies. Rubber and oil palm plantations here are significantly expanding (Aratrakorn *et al.*, 2006; Fitzherbert *et al.*, 2008).

Seventeen meteorological stations were chosen for this study to represent the different geographical and climatological characteristics of the country. The stations include four Northern (N) stations, three Central (C) stations, seven Northeastern (NE) stations and three South East (SE) Coast stations. A map of these stations is listed as Figure 1.

The climate of Thailand is influenced by two major monsoon systems. The area including the N, NE and C stations is referred here as Thai mainland. This region has different climate structure from that of the SE Coast. The NE monsoon brings drier, cooler air from the Chinese mainland causing a dry season from November to mid-March for most of the Thai mainland. This monsoon brings intense weather to the SE Coast. The milder Southwest summer monsoon occurs from mid-May to September. This summer monsoon brings wet air masses from the Indian Ocean causing a wet season over the mainland.

2.2. Data description

Data available from January 1980 to October 2011 covering the 17 stations was used in this study and is detailed below:

Monthly meteorological data was obtained from Thailand Meteorological Department. The data includes average/maximum wind speeds, maximum/minimum temperatures, rainfall and relative humidity. Wind speeds were measured at 9–15 m above ground level.

Standardized ENSO indices, including Multivariate ENSO Index (MEI), SOI, Niño3, Niño4, Niño1+2, Niño3.4, were used. Data was taken from US National Oceanic and Atmospheric Administration, available at http://www.esrl.noaa.gov/psd/data/climateindices/.

The intensity of IOD is represented by Dipole Mode Index (DMI), which is an anomalous sea surface temperature (SST) between the Western Indian Ocean and the Southeastern Indian Ocean. The DMI index was taken from the Japanese Agency for Marine–Earth Science and Technology website (www.jamstec.go.jp).

Level-3 monthly aerosol optical depth (*AOD*) retrieval at 550 nm (MOD08_M3) from Moderate Resolution Imaging Spectroradiometer (MODIS) for years 2000 to 2011 was used. This product has $1^\circ \times 1^\circ$ ($1^\circ \sim 111$ km at the equator) horizontal resolution and was processed using data collected from the Terra satellite. This *AOD* was downloaded from Goddard Earth Sciences Data

and Information Services Center through Giovanni web-based application (http://disc.sci.gsfc.nasa.gov/giovanni/overview/index.html).

Monthly atmospheric optical depths for black carbon and sulphate aerosols used in this study were simulated from the Georgia Institute of Technology–Goddard Global Ozone Chemistry Aerosol Radiation and Transport (GOCART) model. These GOCART aerosol products have spatial resolution of 2° latitude $\times$ 2.5° longitude. For this study, the data were downloaded through Giovanni web-based application and was available for the years 2000–2007.

2.3. Data analysis

2.3.1. Data preparation

Monthly rainfall anomaly was calculated by subtracting the 1980−2011 monthly mean rainfall from the observed rainfall. Spatial MODIS *AOD* and GOCART black carbon and sulphate *AOD*s were extracted to represent information at the studied stations. *AOD* grids covering at the stations were used for the analysis.

The analyses were conducted separately for each of the 4-month intervals. These intervals are as follows: June−August (JJA, representing summer monsoon months), September−November (SON, representing post-summer monsoon months), December−February (DJF, representing dry months for the Thai mainland and wet months for the SE Coast) and March−May (MAM, representing pre-summer monsoon months).

2.3.2. Understanding the common climate structure of Thailand

Each meteorological variable, such as rainfall, may covariate with other variables. These covariations are dependent on season and location. Factor analysis was performed on meteorological measurement data (described in Section 2.2) for different geographical regions under the assumption that the covariations among the observed meteorological variables are influenced by the presence of one or more underlying factors. The analysis estimates uncorrelated underlying factors which are linear combinations of the observed variables. The first factor accounts for the largest eigenvalue, a standardized variance associated with a particular factor, and the higher-order factors are with lesser eigenvalues. Correlation between a factor and an observed meteorological variable is expressed by factor loading. Interpretation of the factors obtained from the factor analysis model could be difficult, thus factor rotation helps to find new factors that are easier to interpret. In this study, Varimax rotation method on a correlation matrix was used. This method is maximizing sum of the variance of the squared loading for each factor. Value of any factors for each observation is called factor score. Investigating the factor loading patterns and spatial–temporal distributions of the factor scores can facilitate understanding the common climate structure of Thailand.

2.3.3. Understanding the connections between ENSO/IOD and Thai rainfall anomalies

In principle, canonical correlation analysis is conducted using two datasets, X and Y, to produce linear combinations (called canonical variables, CANs) of original variables in each X and Y that maximize correlation between them. The first CANs (CAN1) for X and Y yield the highest canonical correlation, whereas the second CANs (CAN2) are later estimated from those yielding the highest correlation and be orthogonal with the previous CAN1. The same rule is applied for higher-order CANs.

To understand the connections between ENSO/IOD and Thai rainfall anomalies, a canonical correlation analysis was performed on monthly rainfall anomalies and ENSO/DMI indices observed from the corresponding month to the previous 12 months. The analysis was conducted using observations from all the stations. The first CAN patterns for the month lag showing the highest canonical correlation were used to determine ENSO and DMI indices, which highly influence the seasonal rainfall anomalies.

2.3.4. Understanding the connections between aerosols and Thai rainfall anomalies

Atmospheric aerosol loading was represented by MODIS-derived *AOD* at 550 nm. This *AOD* was classified into four levels, each containing 25% of total observations. One-way analysis of variance and multiple comparisons using Tukey range test were used to identify significant differences among monthly rainfalls coexisting with the different *AOD* levels. The analyses were conducted separately for each geographical region. For the month intervals observing rainfall–aerosol associations, GOCART black carbon and sulphate *AOD*s were investigated and discussed.

2.3.5. Investigating the usefulness of ENSO/IOD and aerosols for rainfall forecasts

Degrees of rainfall anomalies were classified into five regimes. These rainfall anomalies regimes are near normal (−50, 50 mm), above normal [50, 300), below normal (−100 to −50], extremely above normal [300 and up) and extremely below normal [−100 and less). Long-term (1980−2011) linear trend, ENSO/DMI indices with an appropriate month lag and corresponding *AOD* were used as model predictors to estimate the probabilities of occurring rainfall anomalies in different regimes using linear logistic regression analysis. For each observation, the logistic regression models were estimated using all other observations. The rainfall anomaly regime having the highest probability was chosen and then compared with the observed. The number of observations correctly

predicted using the model to the total number of observations [referred here as correctness ratio (CR)] is calculated. The CR towards one (zero) indicates high (poor) model performance.

3. Results and discussion

3.1. Common climate structure of Thailand

The common climate structure of Thailand was determined through factor analysis of all meteorological variables. Three factors were chosen and their patterns are shown in Table 1.

The first factor is referred here as Wet-factor. High Wet-factor scores ($\geq$0.6), shown in Figure 2, for the Thai mainland stations suggest that high rainfall, along with minimum temperature and relative humidity, were associated with the coming of the Southwestern summer monsoon, which brings moist air from the Indian Ocean to the mainland. For the SE Coast stations, the Wet-factor was positively loaded on monthly rainfall alone and less covariant with the wind speeds and the temperatures, which both are playing roles on local spatial heat exchanges. The rainfall may be formed over the Indian Ocean and brought to the region through regional-scale monsoon systems. High Wet-Factor scores are consistent with the coming of the NE winter monsoon which brings wet air from the Gulf of Thailand to the SE Coast from November to December (Figure 2). This Wet-factor accounts for 19.2–33.6% of total variations of the observations from each geographical group.

The second factor, referred to as the Warm-factor, displays significant positively loading(s) on the minimum and/or maximum temperatures. This Warm-factor accounted for 14.4–22.4% of the total variations. Warm-factor scores were at a maximum before the onset of the Southwest summer monsoon (April for the mainland and May for the SE Coast). The result, shown in Table 1, suggests that monthly fluctuations of nonrainfall-induced warming patterns were mainly explained by the maximum temperature alone for the N, NE and SE Coast regions and both minimum and maximum temperatures for the C region. The insignificant role of the minimum temperature on the fluctuations for the N, NE and SE Coast regions could not be explained in this study.

The third factor is referred to as the Windy-factor. This factor had a significant positively loading on maximum wind speed for all mainland regions and also a loading on the average wind speed for the N and C regions. The time series of Windy-factor scores for each geographical group indicate that the monthly wind speed variations in the mainland are not significantly different from the annual mean. However, Windy-factor scores showed high variations for individual mainland stations suggesting that local forcing(s) should influence wind characteristics. For the SE Coast, high Windy-factor scores indicate high average wind speed and low maximum temperature in December and January, corresponding to the coming of the NE winter monsoon (Figure 2(d)). This Windy-factor accounts for 21.4–25.1% of the total variation.

3.2. Connections of ENSO and IOD with local seasonal rainfall anomalies

Canonical correlation analysis was conducted between 1980–2011 monthly rainfall anomaly and a set of ENSO/DMI indices with different month lags. Patterns of CANs for the month lag yielding the highest canonical correlation are shown in Table 2 and corresponding spatial distributions of canonical correlation coefficients are shown in Figure 3.

Monthly rainfalls exhibited small anomalies (−15.7 to 113.7 mm month^{-1} for 5th to 95th percentile, calculated from total observations from January 1980 to October 2011) for the mainland stations during the local dry season. For the SE Coast stations, December is not dry and the anomalies in DJF were high (−351 to 795 mm month^{-1}, 5th to 95th percentile). These high negative (positive) rainfall anomalies correlated to positive (negative) DMI and negative (positive) SOI, indicating El Niño (La Niña), occurring in the previous 2 months (October–December, OND), as suggested from canonical pattern in Table 2 and moderately high canonical correlation coefficient ($r = 0.31–0.48$) over the SE Coast in Figure 3 (DJF). Moreover, as can be seen in Table 2, both SOI-based ENSO and IOD signals in OND were almost equally weighted. This ENSO–IOD coexistence is consistent with findings from the study on dipole variability of SST in the Indian Ocean conducted by Baquero-Bernal *et al.* (2002). The findings show that in the Indian Ocean from September to November, the ENSO events are primarily associated with dipole-like variability in the SST (Baquero-Bernal *et al.*, 2002). Results from this study further show the connection between this ENSO–IOD coeffects and rainfall anomalies in DJF over the SE Coast of Thailand.

Chansaengkrachang *et al.* (2011) report that strong negative (positive) IOD may cause higher (lower) Thai rainfall in corresponding months based on 1979–2008 monthly rainfall observations. This is simply explained by warm SST anomalies, associated with negative IOD events, in the East of the Indian Ocean which lead to increased evaporation and rain and positive IOD events have the reverse effect (Saji and Yamagata, 2003). This study also observed the relationship between the summer monsoon (in JJA) rainfall and corresponding ENSO signals together with DMI. It was, however, with weaker correlation (overall $r = 0.11$) than that found with the dominant DMI in previous JJA (overall $r = 0.23$). Results from Saji and Yamagata (2003) confirm this weak association over Thailand in the summer monsoon months as suggested by Figure 21 in Saji and Yamagata (2003) which shows low partial correlation of land and SST on DMI independent of Niño3. The findings of this research suggest that even though IOD effect on Thai rainfall was weak in corresponding summer monsoon months, it was still significant despite the response being

Table 1. Factor loading patterns for Wet-, Warm- and Windy-factors for each geographical station group.

Monthly meteorological variables	Wet-factor				Warm-factor				Windy-factor			
	N	C	NE	S	N	C	NE	S	N	C	NE	S
Average wind speed	−0.04	−0.2	−0.1	−0.11	−0.03	0.24	−0.12	0.24	**0.95**	**0.61**	0.49	**0.96**
Maximum wind speed	0.1	0.19	0.21	0.03	0.19	0.06	0.27	0.26	**0.71**	**0.98**	**0.94**	0.07
Maximum temperature	0.05	−0.26	−0.06	−0.37	**0.99**	**0.60**	**0.99**	**0.71**	0.09	0.25	0.01	**−0.60**
Minimum temperature	**0.75**	**0.64**	**0.81**	0.03	0.3	**0.76**	0.27	0.47	0.19	0.06	−0.02	0.01
Rainfall	**0.81**	**0.73**	**0.82**	**0.99**	−0.03	0.02	−0.07	0.05	0.04	0.08	0.04	−0.01
Relative humidity	**0.74**	**0.96**	**0.87**	0.08	0.49	−0.15	−0.43	−0.12	−0.25	−0.18	−0.03	−0.03
Eigenvalue	0.3	0.34	0.36	0.19	0.22	0.17	0.22	0.14	0.25	0.24	0.19	0.22

Values in bold indicate significant correlation (≥0.6) between the factors and the original monthly meteorological variables.

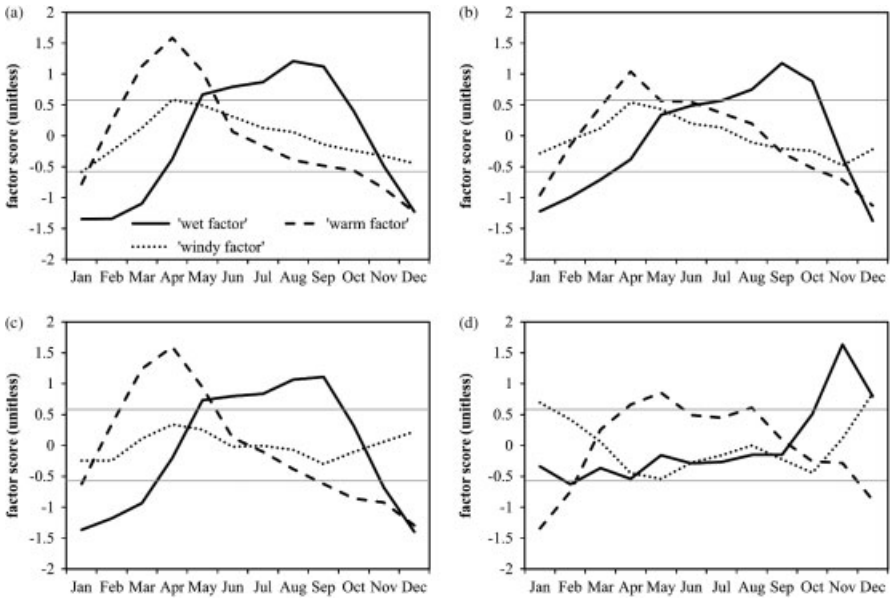

Figure 2. Time series of Wet-, Warm- and Windy-factor scores (detailed in Table 1). The scores outside ±0.6 are significantly different from annual means. (a) Northern Thailand, (b) Central Thailand, (c) Northeastern Thailand and (d) South East Coast Thailand.

delayed and a reverse of the effect. Negative (positive) IOD, relating to a warmer (cooler) Eastern Indian Ocean in summer monsoon months, was associated with less (more) Thai rainfall in the following year's summer monsoon with stronger correlation over the N stations ($r = 0.31–0.38$; Figure 3, JJA). Further study on the long-term response of IOD on summer monsoon rainfall is required to provide greater understanding on the mechanisms responsible for this delayed association. Rainfall anomalies in these summer monsoon months highly fluctuated from −242 to 465 mm month^{-1} (5th to 95th percentile).

This study found that association of the ENSO signals with the summer monsoon rainfall was not significant. Consistent with this conclusion, Singhrattna *et al.* (2005a) show a declining trend of correlation coefficient between June and September rainfall in Thailand and corresponding SOI since 1980. Wang *et al.* (2008) also observed the weakening of the correlation between the summer monsoon and ENSO since the late 1970s and also found more dominant westerly South Asian monsoons, from the northern Arabian Sea to the Philippine Sea, during the El Niño developing phase in JJA. The weakening of the impact associated with warm ENSO events on summer monsoon rainfall was also observed by Ashrit *et al.* (2001) who hypothesized it as a result of enhanced atmospheric moisture and a warmer Eurasian land-mass due to global warming. In addition, the inconsistency of ENSO–summer monsoon response may also be a cause of this weak relationship.

This study found that ENSO was significantly affecting Thai rainfall in the following year's pre- and post-summer monsoon months. Pre-summer monsoon (in MAM) monthly rainfall anomalies fluctuated from −204 to 373 mm month^{-1} (5th to 95th percentile) for the mainland stations and from −137 to 1474 mm month^{-1} (5th to 95th percentile) for the SE Coast stations. As can be seen from the canonical loading pattern for MAM in Table 2, these anomalies clearly relate to all ENSO signals in January to March (JFM). High La Niña signals (negative MEI, Niño1+2, Niño3, Niño4 and Niño3.4 and positive SOI) in JFM were found with high pre-summer monsoon rainfall anomalies with El Niño having the reverse effect. This relationship was more pronounced (overall

Table 2. Correlation coefficients between canonical variable from ENSO/DMI indices and their original variables for month lag yielding the highest overall canonical correlation coefficient.

Months of observed rainfall anomalies	Months of observed ENSO/IOD	Correlation coefficient						
		MEI	SOI	DMI	Niño1 + 2	Niño3	Niño4	Niño3.4
DJF	OND (2 months ago)	0.052	**0.248**	**−0.289**	−0.009	0.004	−0.039	0.036
MAM	JFM (2 months ago)	**−0.709**	**0.781**	−0.235	**−0.569**	**−0.699**	**−0.763**	**−0.790**
JJA	JJA (12 months ago)	0.045	−0.236	**0.752**	−0.219	−0.035	0.118	0.002
SON	MAM (6 months ago)	0.012	**0.561**	−0.172	−0.107	−0.069	0.022	−0.051

'+' and '−' indicate positive and negative correlation with monthly rainfall anomalies, respectively. Bold fonts indicate ENSO/IOD indices highly loading into the canonical variable and they were used in the analysis in Section 3.4.

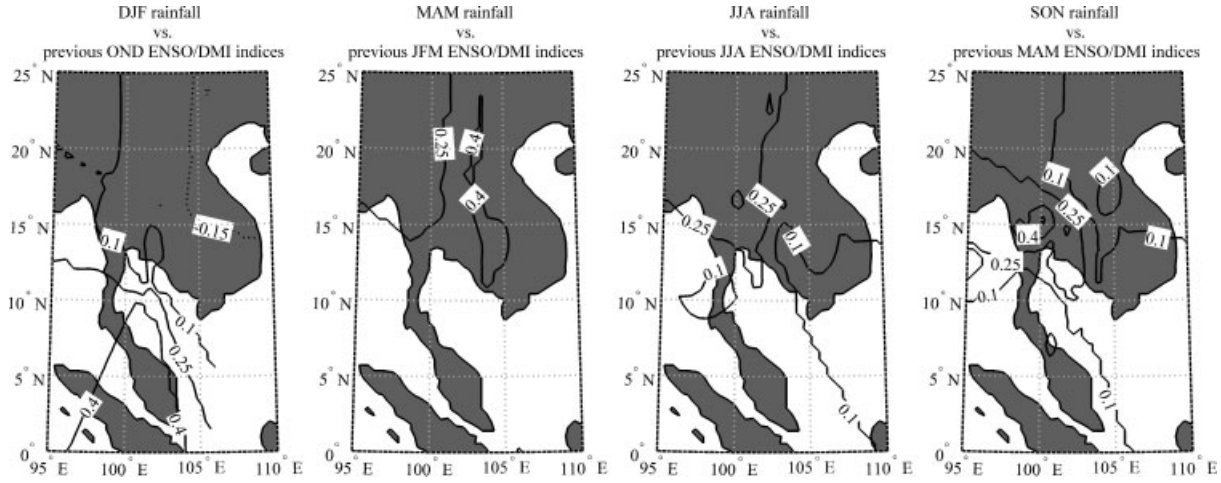

Figure 3. Spatial distribution of canonical correlation coefficient, r, between rainfall anomalies and canonical variable for ENSO and DMI indices with appropriate month lag (see corresponding CAN patterns in Table 2). Contour lines are estimated from kridging interpolation of observations from the 17 stations.

$r = 0.25–0.45$) over the NE. Rainfall anomalies in post-summer monsoon months (in SON) were from −254 to 453 mm month^{-1} (5th to 95th percentile) for the mainland stations and from −496 to 1108 mm month^{-1} (5th to 95th percentile) for the SE Coast stations. The positive (negative) SON rainfall anomalies were likely to be found with positive (negative) SOI, suggesting La Niña (El Niño), 6 months prior to SON. This relationship was stronger over the C station with overall $r = 0.36–0.50$ (Figure 3, SON). Mechanisms governing the associations between ENSO and the following pre- and post-monsoon rainfall should be further investigated.

SOI in OND and MAM was the only ENSO indices showing strong connections with Thai rainfall in DJF and SON, respectively. One reason is possibly a difference in derivation of SOI from the other indices. This SOI is derived from anomalous sea level pressure (SLP) between Tahiti, French Polynesia and Darwin, Australia, whereas all Niño indices are based on anomalous SST. MEI is derived from six observed variables over the tropical Pacific, which included SLP and SST (Hanley *et al.*, 2003). Hanley *et al.* (2003) investigated sensitivities of these ENSO indices on El Niño and La Niña responses and found that SOI is more sensitive to El Niño but less so to La Niña. At first, this study hypothesized that the stronger association with SOI indicated that rainfall in DJF and SON was prone to be affected by El Niño, causing drier weather in Southeast Asia. This hypothesis, however, should be inaccurate; 8 out of the 17 stations showed significant positive rainfall anomaly trends during the DJF and SON. Only one station, Chumphon (in the SE Coast), showed a negative trend in November. At this point, this study can only suggest that SOI is more appropriate for DJF and SON Thai rainfall forecasts. This suggestion is consistent with the findings in the work of Singhrattna *et al.* (2005b) who studied the relationship between multiple ENSO indices and Thai summer monsoon rainfall.

3.3. Connections between seasonal aerosols and local seasonal rainfall

Linear regression analysis shows no significant linear trend of *AOD* from 2000 to 2011. For the N and NE stations, minimum *AOD* was seasonally found from November to December with a maximum in March. For the C stations, the minimum *AOD* was found from July to August with the maximum also being in March. The maximum *AOD* corresponded with a typical biomass burning season over the Southeast Asian mainland (Bridhikitti and Overcamp, 2011). Seasonal aerosol loadings among SE stations did not display a similar pattern. They did, however, tend to be above the

annual mean from February to April, when rainfall is minimized (Figure 1).

The *AOD* observed in approximately $1^\circ \times 1^\circ$ area covering the 17 stations was manually clustered to represent the aerosol loading for each geographical group based on similarities in MODIS *AOD* at 550 nm and GOCART black carbon/sulphate aerosol column ratios. The first group, referred to as 'North Group', includes those at Chiang Mai (N), Nan (N) and Uttaradit (N). The second group, referred to as 'Mixed Mainland Group', includes those at Phisanulok (N), Nakhon Sawan (C) and seven stations in the NE. The third group is referred to as 'Central Group'. It includes those at Lop Buri (C) and Bangkok (C). This Central group is influenced more by coastal conditions than other mainland geographical groups. The fourth group, referred to as 'South Group' includes stations at Chumphon (S), Nakhon Sri Thummarat (S) and Songkhla (S). Monthly rainfalls for different *AOD* levels for four geographical groups are shown in Figure 4.

A significant ($p < 0.01$) decrease in monthly rainfall with increasing *AOD* was observed in pre-summer monsoon months for the North and the Mixed Mainland Groups and in DJF for the South Group. A significant increase in rainfall with increasing *AOD* was observed in post-summer monsoon months for the North and the Mixed Mainland Groups. The aerosol effects during summer monsoon (JJA) and the local dry period (DJF) were not significant for all mainland stations.

As shown in Table 3, rainfall-reducing aerosol had lower sulphate fraction (sulphate *AOD* to total *AOD* column ratio = 0.140−0.456) than those of the rainfall-increasing aerosol (0.614–1.206). Black carbon contents in both aerosols were not significantly different. With lower sulphate content, however, effects of black carbon in rainfall-reducing aerosol may be more pronounced.

Sulphate aerosol has a radiative cooling effect due to its high radiation scattering property (called direct effect) and hence high sulphate aerosol can weaken summer monsoon circulation, thus reducing rainfall (Mitchell and Johns, 1997; Ramanathan *et al.*, 2001). Nonetheless, this aerosol also acts as cloud condensation nuclei, increasing cloud droplets (called indirect effect, Mitchell and Johns, 1997; Ramanathan *et al.*, 2001) and may subsequently increase rainfall. This aerosol, found in SON, may be attributed to coal-fired combustion emissions in the Northern Thailand and/or Southeastern China (Bridhikitti and Overcamp, 2011). Mitchell and Johns (1997) simulated effects of increasing greenhouse gases and sulphate aerosol on future climate. The results suggest less summer monsoon rainfall over Southeast Asia. Their work, however, neglected the indirect effect of the aerosol. Inconsistent with the result from Mitchell and Johns (1997), this study observed that more sulphate aerosol frequently coincided with higher post-summer monsoon rainfall. This suggests that the indirect effect of sulphate aerosol should be incorporated into Southeast Asian rainfall simulations.

Rainfall-reducing aerosols were found in high concentration during pre-summer monsoon months, which are typical during the Southeast Asian biomass burning season. This finding is consistent with that in the work of Jayaraman (2001) showing aerosol-inhibiting rainfall over polluted areas of Thailand and is similar to that observed over the tropical Indian Ocean prior to the onset of the summer monsoon (Jayaraman, 2001). Ma *et al.* (2003) measured biomass burning plumes originating from the Southeast Asian mainland and found aerosols with high water-soluble potassium (K^+) with some sulphate. They also estimated high black carbon emissions over the region. These polluted plumes are observed at altitudes from 2 to 4 km (Ma *et al.*, 2003), being in the range of observed Southeast Asian cloud top layers (Galvin and Walker, 2007). Similar polluted aerosols were also found in Atmospheric Brown Cloud over the Indian Ocean (Stone *et al.*, 2007). Ramanathan *et al.* (2005) simulated summer monsoon rainfall reduction from 1930 to 2000 using observations from the Indian Ocean experiment. It has been estimated from their results that Atmospheric Brown Cloud was responsible for about 8–10% of the rainfall reduction. In this study, rainfall reduction observations made during the pre-summer monsoon season (MAM) showed no significant aerosol effect on summer monsoon rainfall. Aerosol effects observed in this study are similar to the simulating effects of black carbon aerosols on the Indian summer monsoon system in the work of Meehl *et al.* (2008). On the basis of these findings, the biomass burning aerosols can be seen to potentially decrease pre-summer monsoon rainfall over Thai mainland. These aerosols may both absorb and scatter incoming solar radiation thus causing reduction in surface evaporation, weakening latitudinal SST gradients and subsequently causing rainfall reduction (Ramanathan *et al.*, 2005; Meehl *et al.*, 2008).

There was no significant aerosol effects on rainfall level found in the Central Group (Figure 4(c)), including Bangkok station. Particulate pollution in Bangkok is significant and it is attributed to anthropogenic biomass burnings, industrial combustions, automobile emissions and construction (Kim Oanh *et al.*, 2006; Yodsa-nga *et al.*, 2007). This study also found the highest annual mean *AOD* in this Central Group. This high aerosol loading may contribute to significant solar radiation depletion and suppress the precipitation-forming processes (Lensky and Drori, 2007; Yodsa-nga *et al.*, 2007). In fact, lower mean rainfall with higher aerosol loading, indicating rainfall-suppressing aerosol, was found in the Central Group in the post-summer monsoon months (SON) but was not statistically significant due to large standard error (see Figure 4(c)). This rainfall-suppressing property of the Bangkok aerosol is not consistent with satellite detection of positive annual rainfall anomalies over an area downwind of Houston (Texas, USA), which is polluted by emissions from urban activities (Shepherd and Burian, 2003). This high rainfall was hypothesized as being a result of an interaction between an urban heat island convergence and sea-breeze circulation patterns

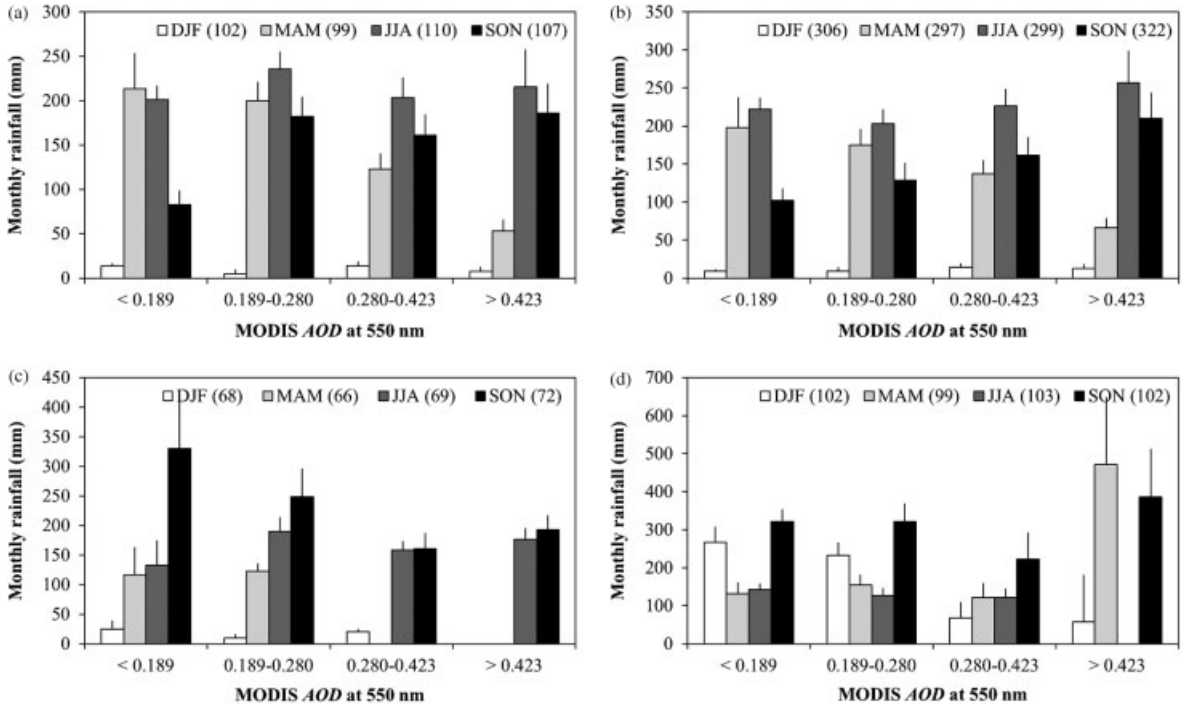

Figure 4. Monthly rainfalls for different MODIS aerosol optical depth (*AOD* at 550 nm) levels for (a) North Group, (b) Mixed Mainland Group, (c) Central Group and (d) South Group. The error bar indicates standard error of the mean and the number in the parenthesis shows the number of observations.

Table 3. Fractions of GOCART black carbon and sulphate aerosol optical depth (*AOD*) on total *AOD* for aerosols associating with decrease and increase in rainfall level.

Geographical group	Rainfall-decreasing aerosols			Rainfall-increasing aerosols		
	Period observed	Black carbon aerosol to *AOD* column ratio	Sulphate aerosol to *AOD* column ratio	Period observed	Black carbon aerosol to *AOD* column ratio	Sulphate aerosol to *AOD* column ratio
North	MAM	0.041–0.088*	0.140–0.317	SON	0.056–0.113	0.780–1.206
Mixed mainland	MAM	0.032–0.050	0.156–0.278	SON	0.046–0.074	0.614–0.930
South	DJF	0.036–0.066	0.263–0.456	–	–	–

*25^{th}–75^{th} percentile.

but the role of aerosol forcing is unclear (Shepherd and Burian, 2003). Van Den Heever and Cotton (2007) conducted a cloud-resolving mesoscale model simulation to investigate the impact of urban aerosol concentrations on convective storm development. They speculated that for urban centres in coastal areas, urban aerosol can have large influences on convective storms and precipitation formation (Van Den Heever and Cotton, 2007). Bangkok has both urban heat island characteristics (Memon *et al.*, 2008) and coastal influences. This coastal environment should enhance turbulent diffusion and advection of local aerosol through sea–land heat exchange. This is suggested in Figure 4(c) which shows no observation having high aerosol loading ($AOD > 0.28$) in the months with relatively high surface temperature (MAM), despite being an active biomass burning season. In addition, the comparison made in this study assumes simultaneous aerosol effect on rainfall, which is not quite appropriate for actual aerosols dynamics. Further study on the relationships and feedback between the aerosol dynamics on downwind precipitation and convection should be conducted for Bangkok and its adjacent areas.

3.4. Implications of ENSO/IOD and aerosols on local seasonal rainfall forecasts

In previous sections, effects of ENSO/IOD and aerosols on local seasonal rainfall have been discussed. This section investigates the usefulness of those dynamics to improve rainfall forecast model performance. Predictor modes used here include the 1980–2011 linear trend, ENSO/IOD signals and seasonal aerosol loading. Linear regression analysis suggests significant rainfall increasing trends (the estimated slope is greater than its standard error) from 1980 to 2011 with the rates ranging from 0.27 mm per 10 years (in Udon Thani, NE station) to 2.2 mm per 10 years (in Nakhon Sri Thummarat, S station). These increases were found in all stations except Mukdahan (−0.6 mm per 10 years). This overall

Table 4. Correctness ratio of logistic regression-based rainfall forecast model using different predictor mode combinations.

	Trend only	Trend + ENSO/IOD	Trend + Aerosol	Trend + ENSO/IOD + Aerosol
Overall	0.33	0.52	0.38	0.65
Individual stations				
Minimum	0.28	0.43	0.32	0.49
Maximum	0.38	0.57	0.48	0.73
Seasons				
DJF	0.24	0.66	0.36	0.77
MAM	0.31	0.45	0.42	0.74
JJA	0.43	0.58	0.43	0.63
SON	0.31	0.39	0.30	0.48
Rainfall regimes				
Near normal	0.41	0.44	0.35	0.56
Above normal	0.41	0.64	0.44	0.74
Below normal	0.02	0.34	0.13	0.50
Extremely above normal	0	0.04	0	0.39
Extremely below normal	0.42	0.63	0.56	0.73

increasing trend is consistent with the observations in the work of Lau and Kim (2006). The aerosol mode was corresponding with the observed rainfall anomalies. This corresponding predictor might not be practical for real-time rainfall forecasts, but it can be useful for scenario-based forecasts. The ENSO/IOD mode used for this forecast was from selected ENSO/DMI indices with appropriate month lags, given in Table 2.

Table 4 shows model CR, which is defined by a ratio of rainfall anomaly regimes that are correctly estimated using a logistic regression model to total number of observations. Using the long-term trend mode only for the forecast yields overall CR of 0.33 with higher value (0.43) for forecast rainfall in summer monsoon months and lower value (0.24) for the DJF forecast. The model poorly forecasted below-normal and extremely above-normal rainfall regimes. This trend mode is linear and it may not capture seasonal variations and interannual epochs of above and below normal rainfalls (Kripalani and Kulkarni, 1997). Introducing ENSO/IOD mode into the forecast model yields better model performance for all cases, especially in DJF (CR = 0.66). Forecast for below-normal rainfall was slightly improved, but was still poor for extremely above-normal case. Introducing individual aerosol mode into the model did not significantly improve model performance (overall CR = 0.38). Model performance was slightly improved for DJF, below-normal and extremely below-normal regimes but near-normal rainfall forecast was slightly poorer.

Interactions among predictor modes should be more attributable to rainfall anomalies than the individual modes. Introducing linear trend, ENSO/IOD and aerosol modes increased overall model CR (0.65) from those without aerosol mode (0.52) in all cases. The performance was markedly high (CR > 0.7) for DJF, MAM, above-normal and extremely below-normal regimes. These findings suggest that ENSO/IOD and aerosols have interactive effects on local seasonal rainfall anomalies in Thailand and ignoring one of them can significantly decrease the effectiveness of rainfall forecast models.

4. Conclusion

Thai climate structure from 1980 to 2011 was investigated from ground measurement data taken from 17 stations. Factor analysis was used to extract underlying seasonal climate structures. Results suggest that high rainfall in rainy season coincided with high minimum temperature and high relative humidity. In the SE Coast region, the rainfall was not strongly associated with other variables. For inland locations, wind speed variation was station-dependent. For the SE Coast, wind speed variations during December and January could be driven by land–sea heat exchanges.

Canonical correlation analysis was used to suggest connections between rainfall anomalies and ENSO/IOD signals with different month lags. Strong ENSO signals found in JFM may affect rainfall in pre-summer monsoon months for the NE and the signals in MAM may affect rainfalls in post-summer monsoon months for the Central (C) region. Effects of ENSO on summer monsoon rainfall were not obvious. Negative (positive) IOD in October, November and December was found with La Niña (El Niño) signal and may be seen to increase (decrease) rainfall in the SE Coast during the months of December, January and February, respectively. Strong IOD events in summer monsoon months may affect rainfall in the North in the following year's summer monsoon season.

AOD at 550 nm taken from MODIS/Terra observations was used to represent atmospheric aerosol loading. Rainfall levels for different aerosol loadings were compared. Results indicate no significant aerosol effect found in the C, despite high background aerosol. A significant decrease in monthly rainfall with increasing *AOD* was observed in pre-summer monsoon months for the deeper inland stations and in DJF for the SE Coast. Significantly increased rainfall with increasing *AOD* was observed in post-summer monsoon months for inland stations. Radiative and hygroscopic (as cloud condensation nuclei) properties of seasonal aerosols should have roles to play in relation to rainfall modifications.

Long-term linear trend (trend mode), ENSO/DMI indices with appropriate month lags (ENSO/IOD mode) and corresponding *AOD* (aerosol mode) were used as model predictors to estimate the probabilities of occurring rainfalls in different rainfall anomaly regimes using linear logistic regression analysis. By introducing ENSO/DMI mode, the forecast model performed better in all cases, compared with those from trend mode only. Individual aerosol mode did not improve the model performance by any significant amount. Interactions among predictor modes should be more attributable to rainfall anomalies than the individual modes. This is suggested from significantly improved model performance when increased amounts of predictors were introduced.

Acknowledgements

This research is supported by the APEC Climate Center under Young Scientist Support Program. The author acknowledges Thailand Meteorological Department for the contribution of ground measurement data used in this study.

References

Aratrakorn S, Thunhikorn S, Donald PF. 2006. Changes in bird communities following conversion of lowland forest to oil palm and rubber plantations in southern Thailand. *Bird Conservation International* **16**: 71–82. DOI: 10.1017/S0959270906000062

Ashrit RG, Kumar R, Kumar KK. 2001. ENSO–summer monsoon relationships in a greenhouse warming scenario. *Geophysical Research Letters* **28**: 1727–1730.

Baquero-Bernal A, Latif M, Legutke S. 2002. On dipolelike variability of sea surface temperature in the tropical Indian Ocean. *Journal of Climate* **15**: 1358–1368.

Bridhikitti A, Overcamp TJ. 2011. Optical characteristics of Southeast Asia's regional aerosols and their sources. *Journal of the Air & Waste Management Association* **61**: 747–754.

Chansaengkrachang K, Aschariyaphotha N, Humphries U, Wangwongchai A, Wongwises P. 2011. Empirical orthogonal function analysis of rainfall over Thailand and its relationship with Indian Ocean Dipole. In *Proceedings of Chiangmai University International Conference 2011*, volume 1, Chiangmai, Thailand, 47–54.

Fitzherbert EB, Struebig MJ, Morel A, Danielsen F, Brühl CA, Donald PF, Phalan B. 2008. How will oil palm expansion affect biodiversity? *Trends in Ecology & Evolution* **23**: 538–545. DOI: 10.1016/j.tree.2008.06.012

Galvin J, Walker M. 2007. Cloudy south-east Asia. *Weather* **62**: 55–56. DOI: 10.1002/wea.5

Hanley DE, Bourassa MA, O'Brien JJ, Smith SR, Spade ER. 2003. A quantitative evaluation of ENSO indices. *Journal of Climate* **16**: 1249–1258.

Jayaraman A. 2001. Aerosol radiation cloud interactions over the tropical Indian Ocean prior to the onset of the summer monsoon. *Current Science* **81**: 1437–1445.

Kim Oanh NT, Upadhyay N, Zhuang Y-H, Hao Z-P, Murthy DVS, Lestari P, Villarin JT, Chengchua K, Co HX, Dung NT, Lindgren ES. 2006. Particulate air pollution in six Asian cities: spatial and temporal distributions and associated sources. *Atmospheric Environment* **40**: 3367–3380. DOI: 10.1016/j.atmosenv.2006.01.050

Kripalani RH, Kulkarni A. 1997. Rainfall variability over South-East Asia – connections with Indian summer monsoon and ENSO extremes: new perspectives. *International Journal of Climatology* **17**: 1155–1168.

Lau KM, Kim KM. 2006. Observational relationships between aerosol and Asian summer monsoon rainfall and circulation. *Geophysical Research Letters* **33**: L21810. DOI: 10.1029/2006GL027546

Lensky IM, Drori R. 2007. A satellite-based parameter to monitor the aerosol impact on convective clouds. *Journal of Applied Meteorology and Climatology* **46**: 660–666. DOI: 10.1175/JAM2487.1

Ma Y, Weber RJ, Lee YN, Orsini DA, Maxwell-Meier K, Thornton DC, Bandy AR, Clarke AD, Blake DR, Sachse GW, Fuelberg HE, Kiley CM, Woo JH, Streets DG, Carmichael GR. 2003. Characteristics and influence of biosmoke on the fine-particle ionic composition measured in Asian outflow during the Transport and Chemical Evolution over the Pacific (TRACE-P) experiment. *Journal of Geophysical Research* **108**: 8816. DOI: 10.1029/2002JD003128

Meehl GA, Arblaster JM, Collins WD. 2008. Effects of black carbon aerosols on the Indian monsoon. *Journal of Climate* **21**: 2869–2882.

Memon RA, Leung DYC, Chunho L. 2008. A review on the generation, determination and mitigation of urban heat island. *Journal of Environmental Sciences* **20**: 120–128.

Mitchell JFB, Johns TC. 1997. On modification of global warming by sulfate aerosols. *Journal of Climate* **10**: 245–265.

Ramanathan V, Crutzen PJ, Kiehl JT, Rosenfeld D. 2001. Aerosols, climate and the hydrological cycle. *Science* **294**: 2119–2124.

Ramanathan V, Chung C, Kim D, Bettge T, Buja L, Kiehl JT, Washington WM, Fu Q, Sikka DR, Wild M. 2005. Atmospheric brown clouds: Impacts on South Asian climate and hydrological cycle. *Proceedings of the National Academy of Sciences of the United State of America* **102**: 5326–5333. DOI: 10.1073/pnas.0500656102

Saji NH, Yamagata T. 2003. Possible impacts of Indian Ocean Dipole mode events on global climate. *Climate Research* **25**: 151–169.

Shepherd JM, Burian SJ. 2003. Detection of urban-induced rainfall anomalies in a major coastal city. *Earth Interactions* **7**: 1–17.

Singhrattna N, Rajagopalan B, Clark M, Kumar KK. 2005a. Seasonal forecasting of Thailand summer monsoon rainfall. *International Journal of Climatology* **25**: 649–664. DOI: 10.1002/joc.1144

Singhrattna N, Rajagopalan B, Kumar KK, Clark M. 2005b. Interannual and interdecadal variability of Thailand summer monsoon season. *Journal of Climate* **18**: 1697–1708.

Stone EA, Lough GC, Schauer JJ, Praveen PS, Corrigan CE, Ramanathan V. 2007. Understanding the origin of black carbon in the atmospheric brown cloud over the Indian Ocean. *Journal of Geophysical Research* **112**: D22S23. DOI: 10.1029/2006JD008118

Van Den Heever SC, Cotton WR. 2007. Urban aerosol impacts on downwind convective storms. *Journal of Applied Meteorology and Climatology* **46**: 828–850. DOI: 10.1175/JAM2492.1

Walker A. 2002. Forests and water in Northern Thailand. *Chiangmai University Journal* **1**: 215–242.

Wang B, Yang J, Zhou T, Wang B. 2008. Interdecadal changes in the major modes of Asian–Australian monsoon variability: strengthening relationship with ENSO since the late 1970s. *Journal of Climate* **21**: 1771–1789.

Yodsa-nga P, Boonyawat S, Udomchoke V, Aungsuratana P. 2007. The influence of atmospheric aerosol on solar radiation degradation in each region of Thailand. *Kasetsart Journal (Natural Science)* **41**: 601–610.

